Transmural Gradients in Na/K Pump Activity and $[Na^+]_i$ in Canine Ventricle

J. Gao, W. Wang, I. S. Cohen, and R. T. Mathias
Department of Physiology & Biophysics, State University of New York at Stony Brook, Stony Brook, NY

ABSTRACT There are well-documented differences in ion channel activity and action potential shape between epicardial (EPI), midmyocardial (MID), and endocardial (ENDO) ventricular myocytes. The purpose of this study was to determine if differences exist in Na/K pump activity. The whole cell patch-clamp was used to measure Na/K pump current (I_P) and inward background Na^+-current (I_{inb}) in cells isolated from canine left ventricle. All currents were normalized to membrane capacitance. I_P was measured as the current blocked by a saturating concentration of dihydro-ouabain. $[Na^+]_i$ was measured using SBFI-AM. I_P(ENDO) (0.34 ± 0.04 pA/pF, $n = 17$) was smaller than I_P(EPI) (0.68 ± 0.09 pA/pF, $n = 38$); the ratio was 0.50 with I_P(MID) being intermediate (0.53 ± 0.13 pA/pF, $n = 19$). The dependence of I_P on $[Na^+]_i$ or voltage was essentially identical in EPI and ENDO (half-maximal activation at 9–10 mM $[Na^+]_i$ or ~−90 mV). Increasing $[K^+]_o$ from 5.4 to 15 mM caused both I_P(ENDO) and I_P(EPI) to increase, but the ratio remained ~0.5. I_{inb} in EPI and ENDO were nearly identical (~0.6 pA/pF). Physiological $[Na^+]_i$ was lower in EPI (7 ± 2 mM, $n = 31$) than ENDO (12 ± 3 mM, $n = 29$), with MID being intermediate (9 ± 3 mM, $n = 22$). When cells were paced at 2 Hz, $[Na^+]_i$ increased but the differences persisted (ENDO 14 ± 3 mM, $n = 10$; EPI 9 ± 2 mM, $n = 10$; and MID intermediate, 11 ± 2 mM, $n = 9$). Based on these results, the larger I_P in EPI appears to reflect a higher maximum turnover rate, which implies either a larger number of active pumps or a higher turnover rate per pump protein. The transmural gradient in $[Na^+]_i$ means physiological I_P is approximately uniform across the ventricular wall, whereas transporters that utilize the transmembrane electrochemical gradient for Na^+, such as Na/Ca exchange, have a larger driving force in EPI than ENDO.

INTRODUCTION

The T wave of the electrocardiogram is generated by transmural differences in the action potential waveform (1). As shown in the left-hand panel of Fig. 1, the epicardial (EPI) action potential has a ''spike and dome'' morphology. The ''spike'' is initiated by the fast Na^+-current, which is rapidly followed by a large transient outward K^+-current called I_{to1}. The onset of I_{to1} causes a negative voltage deflection, giving the appearance of a ''spike,'' then its inactivation causes depolarization, which gives the plateau phase of the EPI action potential its ''dome'' appearance. As shown in the right-hand panel of Fig. 1, the endocardial (ENDO) action potential is longer and does not display a prominent spike or dome (2). This difference is at least in part due to a reduced density of I_{to1}, which also has slower recovery from inactivation in ENDO than EPI myocytes (3). The presence of I_{to1} with different properties in the two cardiac regions has a number of functional consequences including a greater adaptation of the EPI action potential waveform to rate, and a differential sensitivity of the two cell types to ischemia, pharmacologic agents, and elevated $[K^+]_o$ (2).

In addition to differences between EPI and ENDO, the action potential in midmyocardial (MID) myocytes has the spike-and-dome morphology but is longer in duration than that in either EPI or ENDO. This appears to be due to a smaller amplitude slow-activating K^+-current, I_{Ks} (4), and a larger amplitude slower-inactivating late Na^+-current (5). Moreover, the differences in action potential waveform must also, by necessity, lead to differences in the activation of all other membrane currents that flow during the plateau. This includes the slowly inactivating Na^+-current, and the L-type Ca^{2+}-current. It is a balance of these passive movements of ions down their electrochemical gradients and the active restorative processes (the Na/K pump, and the Na/Ca exchanger) that determine resting levels of Na^+ and Ca^{2+} and thus regional differences in contractile strength. The purpose of this investigation was to determine whether the chronic differences in ionic currents are associated with transmural differences in Na/K pump activity. This work was previously reported in abstract form (6).

METHODS

Single myocytes were enzymatically isolated from EPI, MID, and ENDO regions of the left ventricular free wall. Small cubes (1–1.5 mm on a side) were dissected from EPI and ENDO. For MID myocytes, the ~1-cm-thick wall was dissected into thirds, then 1–1.5-mm cubes were dissected from the middle third (7–8). Isolated cells were stored in KB solution containing KCl, 83 mM; K_2HPO_4, 30 mM; $MgSO_4$, 5 mM; Na-Pyruvic Acid, 5 mM; b-OH-Butyric Acid, 5 mM; Creatine, 5 mM; Taurine, 20 mM; Glucose, 10 mM; EGTA, 0.5 mM; KOH, 2 mM; and Na_2-ATP, 5 mM, at pH = 7.2.

Cells were placed in a temperature-controlled Lucite bath (32 ± 0.5°C). An Axopatch 1A amplifier (Axon Instruments, Union City, CA) and the whole-cell patch-clamp technique were employed to observe cell membrane current. Patch-pipette resistances were 1–3 M Ω before sealing. The pipette solution contained Na-Aspartic Acid, 50 mM; K-Aspartic Acid, 20 mM; CsOH, 30 mM; TEACl, 20 mM; NaH_2PO_4, 10 mM; HEPES, 5 mM; EGTA, 11 mM; $CaCl_2$, 1 mM (except where stated); Glucose, 10 mM; and Mg-ATP, 5 mM, at pH = 7.2 adjusted with CsOH. The external Tyrode solution contained NaCl, 137.7 mM; NaOH, 2.3 mM; $MgCl_2$, 1 mM; KCl, 5.4 mM

Submitted March 7, 2005, and accepted for publication June 2, 2005.

Address reprint requests to R. T. Mathias, Tel.: 631-444-3041; Fax: 631-444-3432; E-mail: richard.mathias@sunysb.edu.

0006-3495/05/09/1700/10 $2.00

doi: 10.1529/biophysj.105.062406

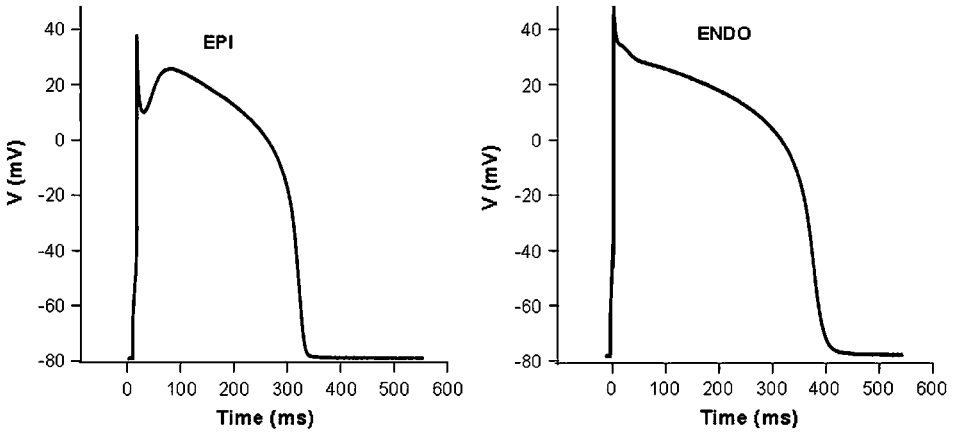

FIGURE 1 A comparison of action potentials in ENDO and EPI myocytes. Action-potential waveforms were recorded in isolated myocytes using the whole-cell patch-clamp technique. The left-hand panel shows a typical EPI action potential with its ''spike and dome'' morphology. In contrast, as shown in the right-hand panel, ENDO action potentials are longer in duration and lack the spike-and-dome.

(except where stated); $CaCl_2$, 2 mM; glucose, 10 mM; HEPES, 5 mM; $BaCl_2$, 2 mM; and $CdCl_2$, 1 mM, at pH = 7.4. Different values of $[Ca^{2+}]_o$ were added when necessary.

Whole-cell patch-clamp recordings

Myocytes were held at 0 mV, and 1 mM dihydro-ouabain (DHO) was added to the external solution to block the Na/K pump current (I_P). To investigate the I_P–V_m relationship, a 4-s voltage ramp was applied from +50 to −100 mV. Cell membrane capacitance was measured in the current clamp mode by applying a −50 pA current step and observing the membrane potential change. The pump current density was obtained by normalizing the current to the cell's membrane capacitance. In the experiments to measure the inward background current, E_K and E_{Cl} were set to −60 mV by modifying $[K^+]$, $[Cs^+]$, [Aspartic Acid$^-$], and $[Cl^-]$ in the pipette solution. The free $[Ca^{2+}]$ was calculated from the SPECS program (9,10). All patch-clamp data were recorded on computer disk for later analysis. Results are given as mean ± SD. When only ENDO and EPI myocytes were studied, statistical significance was determined by the Student's *t*-test, and $p < 0.05$ was considered a significant difference between two sets of data. When EPI, MID, and ENDO myocytes were compared, one-way analyses of variance were used to test the effect of cell position (EPI, MID, and ENDO) on Na/K pump current and intracellular sodium (quiescent and 2 Hz). Whenever there was a statistically significant effect of cell position, post-hoc tests (Tukey's honestly significant difference) were used to determine which pair of means significantly differed.

Measurement of $[Na^+]_i$

$[Na^+]_i$ was measured as described in Diarra et al. (11) and Despa et al. (12). Myocytes were loaded with SBFI-AM (10 μM) for 60 min at room temperature. Pluronic F-127 (0.2% w/v) was used to facilitate loading. Myocytes were then washed in normal Tyrode solution for 20 min to ensure de-esterification of the SBFI-AM to SBFI. They were next placed in a perfusion chamber (32°C) on a Nikon Diaphot-TMD inverted fluorescence microscope equipped with an LWD Fluor-60× objective lens (Nikon, Tokyo, Japan). Excitation from a Xenon 75-W lamp was passed through 340-nm and 380-nm filters, which were alternated using a Lambda 10-2 filter wheel (Sutter Instrument, Novato, CA). Emission was collected at 510 nm using an intensifier-coupled Retiga EX 6864 CCD camera (Q-Imaging, Burnaby, BC, Canada). A typical cell is shown in Fig. 2 *A*. This cell was from ENDO; however, ENDO, MID, and EPI cells were physically indistinguishable. Background fluorescence was corrected before the ratio was calculated. Ratio pairs were collected at 10-s intervals to minimize photobleaching. Autofluorescence was undetectable.

The calibration curve (Fig. 2 *B*) was measured as described above but with myocytes incubated in media containing six different $[Na^+]$ values (0–30 mM), 10 μM gramicidin, and 100 μM strophanthidin. The curve was normalized to its value at $[Na^+]_i$ = 10 mM, then after each experimental determination of $[Na^+]_i$, a single point calibration was done at 10 mM $[Na^+]_i$ (11) and the experimental ratio was normalized and compared to the normalized calibration curve. The calibration data were fit to the standard model for binding of Na^+ with SBFI causing an increase in fluorescence emission when excitation was at 340 nm, but not when excitation was 380 nm. In this situation, the ratio, *R*, of emission at 340-nm excitation to that at 380 nm is described by

$$R = \frac{R_{min}K + R_{max}[Na^+]_i}{K + [Na^+]_i}.$$

The best-fit values were $R_{min} = 0.81$, $R_{max} = 3.06$, and $K = 98.5$ mM. The tested values of $[Na^+]_i$ were limited to the low range of the binding curve, so the projected value of R_{max} is unlikely to be very accurate. Nevertheless, the curve provides a good fit to the data over the range studied, so it should accurately relate experimental values of *R* to $[Na^+]_i$ in the physiological range. The dashed lines indicate the experimental values of *R* and predicted $[Na^+]_i$ determined in quiescent cells from ENDO and EPI regions of the canine left ventricle.

RESULTS

Transmural differences in I_P

All of our membrane current measurements were normalized to cell capacitance. Fig. 3 *A* illustrates how capacitance was measured. A current step of −50 pA was applied to a myocyte and the voltage response recorded. There was an initial voltage jump due to the pipette resistance (see Fig. 3, *inset*). This jump divided by the applied current gave the pipette tip resistance. Subsequently, the voltage changed along an exponential time-course. The amplitude of the exponential voltage response divided by the applied current gave the input resistance (R_{in}), which in this case was 270 MΩ. The time constant of the voltage response divided by R_{in} gave the cell capacitance (C_m), which was 222 pF for this myocyte. The mean C_m for ENDO myocytes was 202 ± 45 pF (n = 11) and for EPI myocytes was 189 ± 36 pF (n = 15). These two values did not differ significantly ($p > 0.05$).

In a previous study of canine and guinea pig ventricular myocytes (13) we demonstrated that 1 mM DHO was essentially saturating and blocked >95% of total I_P. We therefore

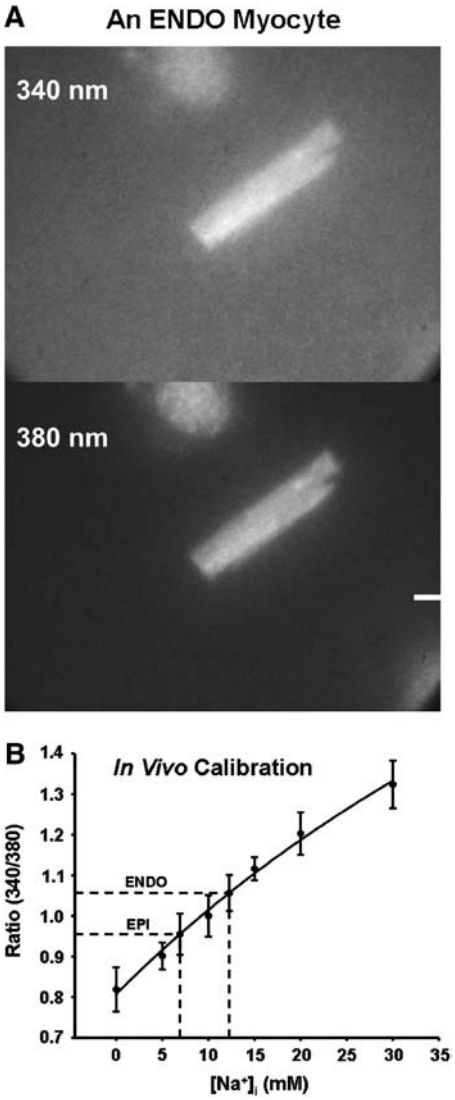

FIGURE 2 The method of measuring $[Na^+]_i$. (*A*) An isolated ENDO myocyte loaded with SBFI and illuminated with 340-nm or 380-nm light. The background fluorescence seen here was subtracted from the cell fluorescence before calculating the ratio. (*B*) An in-cell calibration curve relating the ratio of fluorescence at 340-nm and 380-nm excitation to known $[Na^+]_i$. The curve was recorded and analyzed as described in the text. The dashed lines show the values of the ratio recorded in quiescent cells from either EPI or ENDO and the corresponding values of $[Na^+]_i$.

began our study of ENDO and EPI myocytes by clamping the membrane potential to 0 mV and adding 1 mM DHO to the perfusate to measure total pump current. Fig. 3 *B* shows sample records for EPI and ENDO myocytes. Un-normalized total pump current (indicated by the *dashed lines*) is the change in current in response to application of 1 mM DHO. In these two examples, un-normalized pump current was 119 pA in the EPI myocyte and 65 pA in the ENDO myocyte. C_m was 198 pF in EPI and 187 pF in ENDO myocytes, yielding normalized pump currents, I_P, of 0.60 pA/pF and 0.35 pA/pF, respectively. The results of this experimental protocol for the entire population of EPI, MID, and ENDO myocytes are illustrated in Fig. 3 *C*. The mean I_p(EPI) was 0.68 ± 0.09 pA/pF (38 cells from seven dogs), I_P(MID) was 0.53 ± 0.13 pA/pF (19 cells from four dogs), and I_P(ENDO) was 0.34 ± 0.04 pA/pF (17 cells from four dogs). The effect of position on I_P was tested using a one-way analysis of variance and was found to be significant ($p < 0.001$). Mean I_P at one location (EPI, MID, or ENDO) was compared to other locations. All such comparisons showed significant differences ($p < 0.001$). Thus there is a transmural gradient in I_p: I_P in ENDO is smaller than in EPI myocytes, with the ratio being 0.50.

The DHO-affinity and $[K^+]_o$-activation of I_P

Although our previous studies demonstrated that >95% of total I_P was blocked by 1 mM DHO in canine ventricular myocytes, only EPI myocytes were included in those studies. We therefore considered the possibility that Na/K pumps in ENDO myocytes have a lower affinity for DHO. We tested this alternative by measuring I_P in response to application of 2 mM DHO. If the DHO-affinity of the Na/K pumps was lower in ENDO, the difference between the DHO-sensitive current between the two types of myocytes should be reduced. The results are shown in Fig. 4 *A*. I_p(ENDO) was 0.30 ± 0.12 pA/pF ($n = 12$) and I_P(EPI) was 0.63 ± 0.09 pA/pF ($n = 8$), and the ratio was 0.48. Thus the difference in I_p(EPI versus ENDO) is not due to a difference in DHO affinity.

All of our results up to this point were obtained with $[K^+]_o$ of 5.4 mM. If the $[K^+]_o$-affinity of Na/K pumps was lower in ENDO than EPI myocytes, a difference in I_p would be observed. We tested this alternative by raising $[K^+]_o$ to 15 mM. The results are illustrated in Fig. 4 *B*. The average I_p(EPI) increased to 0.82 ± 0.20 pA/pF ($n = 6$), and the average I_P(ENDO) increased to 0.38 ± 0.12 pA/pF ($n = 8$), but the ratio was still ~0.5. Thus a difference in $[K^+]_o$-affinity cannot account for the difference in I_P.

These data also suggest that accumulation/depletion of external K^+ in restricted spaces is not a significant source of error in our determination of I_P. The solutions used for these experiments blocked virtually all K^+-channel activity, leaving I_P as the major source of K^+-transport. If I_P caused K^+-depletion in the T-system or other restricted extracellular compartments, then the depletion should have been greater in EPI than ENDO myocytes. This would have caused an underestimate of the difference between I_P(EPI) and I_P(ENDO). In this situation, the ratio of I_P(ENDO)/I_P(EPI) in 15 mM $[K^+]_o$ should have changed from that in 5.4 mM $[K^+]_o$, but it did not. Thus, external K^+ accumulation/depletion does not seem to be a significant problem when measuring I_P in isolated myocytes under these conditions.

The voltage-dependence of I_P

The previous results were all obtained at a holding voltage of 0 mV, so it was possible that a difference in voltage dependence generated the difference in I_P between ENDO and EPI

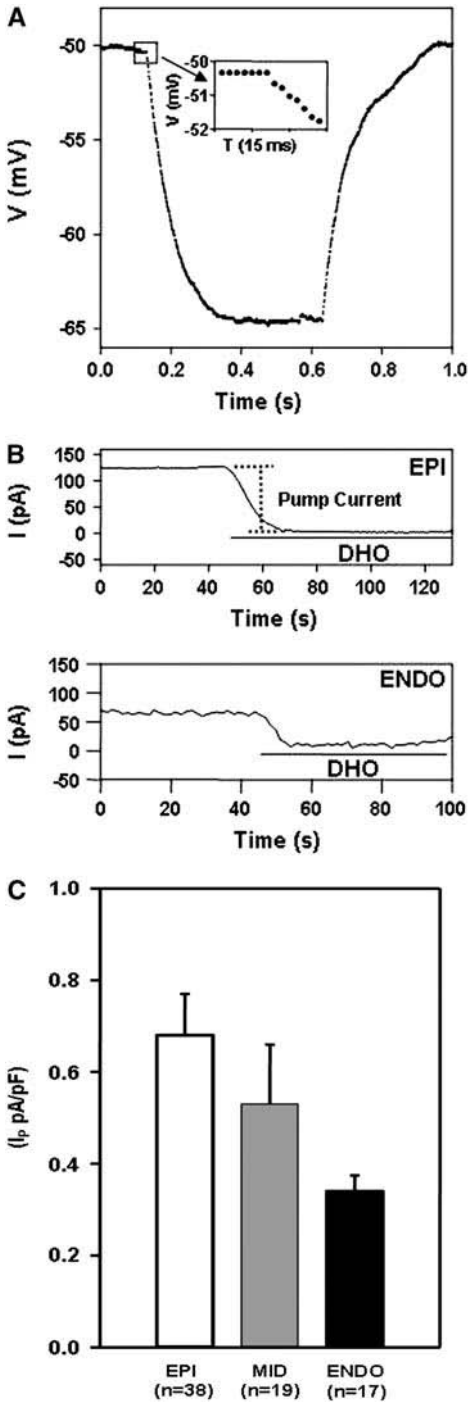

FIGURE 3 A comparison of I_P in EPI, MID, and ENDO myocytes. To control for differences in cell size, input capacitance was measured, then I_P was normalized to this capacitance. The units of I_P (*pA/pF*) should be close to $\mu A/cm^2$, assuming a specific membrane capacitance of 1 $\mu F/cm^2$. Total pump current (*pA*) was measured as the current blocked by 1 mM DHO. It was divided by total capacitance, and I_P from EPI and ENDO myocytes was estimated. (*A*) The protocol to measure cell membrane capacitance. The membrane potential response to a −50 pA current pulse with duration of 500 ms was recorded. The insert indicates the initial voltage jump due to the pipette series resistance. The time constant (τ) could be measured from the time-dependent voltage response after the initial jump. Input resistance, R_{in} = (*the total voltage response minus the voltage jump*)/50 pA, and cell capacitance = τ/R_{in}. (*B*) The measurement of I_P. A myocyte was held at 0 mV. After the holding current reached steady state, the bathing solution was switched to one containing 1 mM DHO, which induced an inward shift in holding current. The difference in the holding current before and after DHO application represents the estimated total pump current. Pump current density I_P = total pump current/cell membrane capacitance. Upper-panel record was obtained from an EPI myocyte and the lower-panel record was from an ENDO myocyte. (*C*) I_P in EPI myocytes is larger than that in ENDO myocytes with MID being intermediate. I_P was measured as described in *B*. The number of cells observed was *n*, and error bars indicate standard deviations. The ratio of I_P(ENDO)/I_P(EPI) was 0.50.

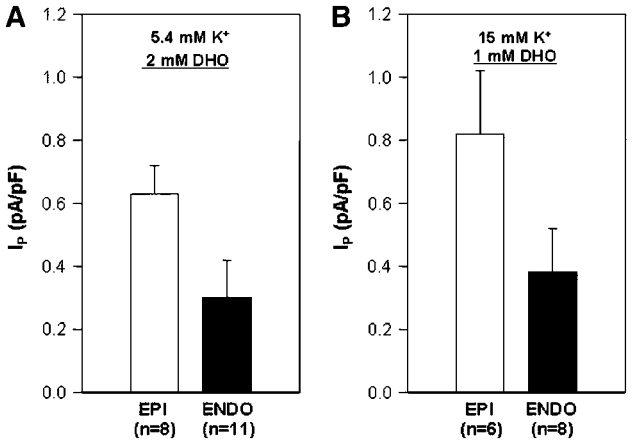

FIGURE 4 The DHO-affinity and $[K^+]_o$-activation of I_P. The larger value of I_P(EPI) than I_P(ENDO) could be explained by an unusually low DHO-affinity or $[K^+]_o$-activation of I_P(ENDO). (*A*) To test that 1 mM DHO was saturating for Na/K pumps from both types of myocytes, 2 mM DHO was applied in these experiments with an external K^+ concentration of 5.4 mM. The number of cells observed was *n*, and error bars indicate standard deviations. I_P determined with 2 mM DHO was indistinguishable from that shown in Fig. 1 *C* determined using 1 mM DHO, suggesting that either concentration was saturating (I_P(EPI) differs from I_P(ENDO), $p \leq 0.01$). (*B*) I_P was measured using 1 mM DHO with an external solution containing 15 mM $[K^+]_o$. The number of cells observed was *n*, and the error bars indicate standard deviations. In comparison to measurements in 5.4 mM $[K^+]_o$, I_P in either type of myocyte was larger, consistent with the $[K^+]_o$-affinity previously measured (13,20). However, the ratio of I_P(ENDO)/I_P(EPI) remained 0.46, the same as in 5.4 mM $[K^+]_o$, suggesting little or no difference in $[K^+]_o$-affinity for the Na/K pumps from ENDO and EPI myocytes. As described in the text, these data also suggest that accumulation/depletion of external K^+ in restricted spaces is not a significant source of error in our determination of I_P. (I_P(EPI) differs from I_P(ENDO), $p \leq 0.01$.)

myocytes. Our results on the voltage dependence of I_P are shown in Fig. 5. The myocytes were held at 0 mV, then a voltage ramp from +50 mV to −100 mV was applied in a 4-s period. Sample voltage and current records are provided in Fig. 5 *A*. The ramps were applied both in the absence and presence of 1 mM DHO. Fig. 5 *B* shows *I–V* relationships from an EPI myocyte for each of these conditions, as well as the difference current (obtained by subtracting the average of 10 I_m–V_m curves in the presence of DHO from the average of 10 I_m–V_m curves before DHO application). Fig. 5 *C* shows average data from five EPI and five ENDO myocytes along

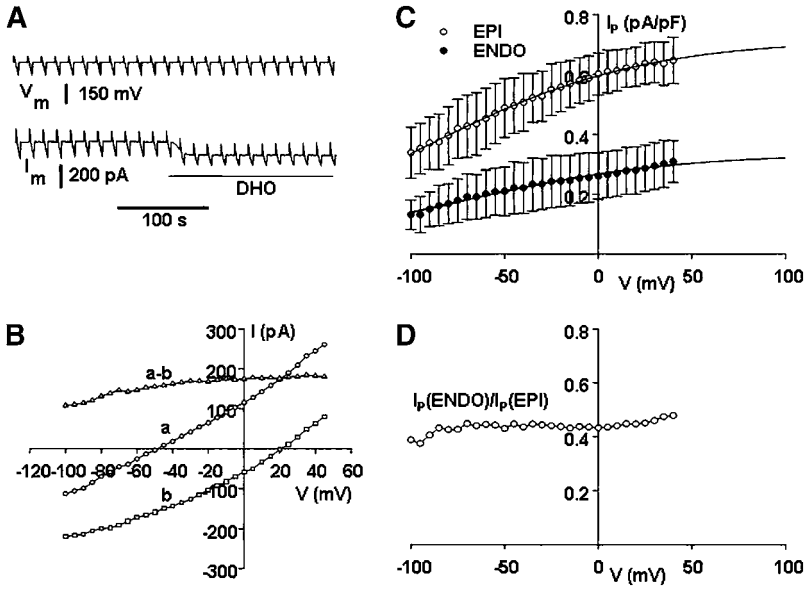

FIGURE 5 The voltage-dependence of I_P. Previous studies were all done at a membrane voltage of 0 mV. Thus, if the voltage-dependence of I_P(EPI) was significantly different than that of I_P(ENDO), it would not have been detected and could have caused the observed difference. (*A*) The protocol for measuring the cell's current-voltage response. V_m and I_m are the voltage and the current recordings. A myocyte was held at 0 mV and a voltage ramp with a range of 50 to −100 mV and duration of 4 s was delivered before and during DHO application. A total of 10 ramps were applied in each condition and the currents were averaged. (*B*) An example of *I–V* curves obtained from a single cell. The *I–V* relationships were constructed from data sampled at a rate of 40 ms/point, filtered at 2 KHz, and analyzed at 5-mV intervals by averaging points within a ±2.5 mV window. Curves *a* and *b* are the average I_m–V_m relations from this cell recorded before and during DHO application, respectively. Each curve is averaged from 10 I_m–V_m curves recorded in each condition. Curve *a–b* is the un-normalized I_p–V_m relationship, obtained by subtracting the average I_m–V_m relationship recorded in *a* (the presence of 1 mM DHO) from that obtained in *b* (the absence of DHO). (*C*) The average voltage-dependence of I_P in EPI and ENDO myocytes. The I_P–V_m relationships were constructed by normalizing I_P to the cell's membrane capacitance. The I_P–V_m relationships from EPI (*open circles*) and ENDO (*solid circles*) are each an average from five cells. Error bars indicate standard deviations. The smooth curves were obtained by curve-fitting as described in the text. (*D*) The ratio of I_P(ENDO)/I_P(EPI). The ratio was calculated from the I_P–V_m data in *C*. It is relatively constant at a value ~0.44 across the entire 150-mV range studied, indicating no significant difference in the voltage dependence of I_P in the two cell types.

with the standard deviation at each potential. Both data sets were fit by the function

$$I_P = I_{max}/(1 + e^{-\phi}),\ \phi = \sigma(V_m - V_{1/2})F/RT,$$

where I_{max} is the maximal value of I_P (at V_m = infinity), V_m is the membrane potential, $V_{1/2}$ is the membrane potential at which I_P reaches the half-value of I_{max}, and σ is a factor between 0 and 1 representing the slope of the voltage dependence of I_P at $V_{1/2}$. I_{max} was 0.71 pA/pF in EPI and 0.33 pA/pF in ENDO, $V_{1/2}$ was −92 mV in EPI and −89 mV in ENDO, and σ was near unity in both cell types. We also plotted the ratio I_P(ENDO)/I_p(EPI) at each voltage, and this is displayed in Fig. 5 *D*. There is little or no change in this ratio (0.44 ± 0.02) over the entire 150-mV range studied. Thus the voltage-dependence of I_P is essentially identical in EPI and ENDO myocytes, and cannot account for the larger I_P observed in EPI.

I_{inb} and the $[Na^+]_i$-dependence of I_P

The larger I_P in EPI than ENDO myocytes was unlikely to be due to differences in $[Na^+]_i$-activation, since the whole-cell pipette contained 60 mM Na^+, which should have resulted in a value of $[Na^+]_i$ that was saturating for I_P (13). Nevertheless, this possibility was tested. Moreover, we were interested in physiological conditions, where the larger maximum I_P in EPI could result in lower $[Na^+]_i$, depending on Na^+-influx and the $[Na^+]_i$-dependence of I_P in the two types of myocytes.

Fig. 6 *A* shows the protocol we used to estimate both the dependence of I_p on $[Na^+]_i$ and the magnitude of I_{inb}. To eliminate contributions of K^+- and Cl^--currents, we set $E_K = E_{Cl} = -60$ mV, which was our holding potential for these experiments. Under these conditions, the major remaining currents should be un-normalized versions of I_P and I_{inb}. As shown in Fig. 6 *A*, total pump current was blocked with 1 mM DHO (*shorter vertical bar*) leaving the total inward background Na^+-current, as indicated by the larger vertical bar. As a control, external Na^+ was replaced with choline to verify that the major current source was inward Na^+-current. Since zero $[Na^+]_o$ might affect DHO inhibition of I_P, we tested the effect of 1 mM versus 2 mM DHO in the same cell with $[Na^+]_o = 0$ mM. The ratio of pump currents I_P(DHO = 2 mM)/I_P(DHO = 1 mM) was 0.99 ± 0.23 ($n = 6$), indicating that either concentration was saturating for inhibition of I_P. If choline were totally impermeant, the current should go to near-zero, but slightly outward due to a small Na^+-efflux from the cell (see the estimate below). In reality, the current is near zero, but slightly inward. This residual inward current is possibly due to a small permeability for choline or it may be due to E_K, E_{Cl}, and V_m not being at precisely the same value. Whatever the cause, it should not generate a large error in our estimate of I_{inb}. The protocol shown Fig. 6 *A* was repeated in at least five cells for each concentration of pipette Na^+, thus providing the dependence of both I_P and I_{inb} on $[Na^+]_P$, but as described in Mathias et al. (14) and measured by Gao et al. (13), $[Na^+]_i$ generally differs significantly from $[Na^+]_P$.

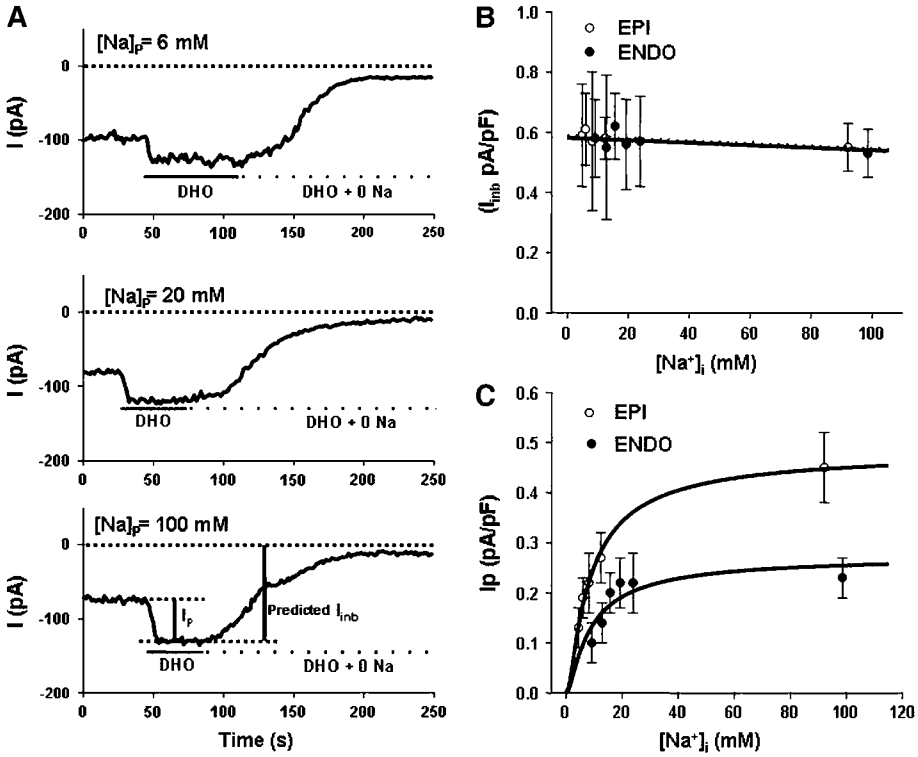

FIGURE 6 I_{inb} and the $[Na^+]_i$-dependence of I_p. Previous measurements of I_P in EPI and ENDO were made with the same pipette $[Na^+]$ of 60 mM. It was possible that $[Na]_i$-activation of I_P in EPI was different than in ENDO myocytes, causing the difference in I_P. Moreover, because $[Na]_i$ is far from equilibrium, I_{inb} depends very little on $[Na]_i$, whereas I_P depends strongly on physiological values of $[Na]_i$. A myocyte achieves steady-state by adjusting $[Na]_i$ until Na^+ influx and efflux are the same. The $[Na]_i$-dependence of I_P and the value of I_{inb} are therefore of intrinsic physiological interest. (*A*) I_P and I_{inb} measured in a single ENDO myocyte. In these experiments, E_K and E_{Cl} were set to −60 mV and the cells were voltage-clamped to −60 mV to eliminate K^+- or Cl^--currents. In addition, the external solution contained 2 mM Ba^{2+} to block K^+-channels and 1 mM Cd^{2+} to block Ca^{2+}-channels and Na/Ca exchange. In this condition, the Na/K pump current and the inward background Na^+-current should be all that remains. Application of 1 mM DHO should remove the pump current and leave only the inward background Na^+-current. If so, then removal of external Na^+ should cause the total current to go to near zero, which it did. The vertical bars in the bottom graph represent un-normalized I_P and I_{inb}. In the upper panel, un-normalized I_P was 30 pA and I_{inb} was 128 pA at 6 mM $[Na]_p$. In the middle panel, un-normalized I_P was 41 pA and I_{inb} was 122 pA at 20 mM $[Na^+]_P$. In the bottom panel, un-normalized I_P was 56 pA and I_{inb} was 130 pA at 100 mM $[Na^+]_P$. (*B*) The $[Na^+]_i$–dependence of I_{inb}. The open circles represent I_{inb} in EPI myocytes and the solid circles in ENDO myocytes. Error bars indicate standard deviations. The dashed and solid lines are the best fit of the constant field equation (see text) for EPI and ENDO myocytes, respectively. I_{inb} was virtually identical in the two types of cells and weakly dependent on $[Na]_i$. (*C*) The $[Na^+]_i$-dependence of I_P. The open and the solid circles represent I_P(EPI) and I_P(ENDO), respectively. The smooth curves are the best fit with a model of three independent and identical Na^+-binding sites (see text). The ratio of I_{max} ENDO/EPI was 0.56 but the values of half-saturating $[Na^+]_i$ were virtually identical, being between 9 mM and 10 mM for either type cell.

The difference between bulk $[Na^+]_i$ and $[Na^+]_P$ occurs whenever there is net steady-state Na^+-flux across the plasma membrane. In this condition there must be an equal steady-state Na^+-flux between pipette and cell, and diffusion of Na^+ between pipette and cell requires a concentration difference between the bulk pipette-Na^+ and intracellular-Na^+, with the concentration change occurring within the pipette very near the tip (14). In the present studies, net transmembrane Na^+-flux (moles/cm^2/s) has been measured and is given by $(3I_P - I_{inb})/F$, where F (10^5 Coulombs/mole) is the Faraday constant and values of current reported in pA/pF are assumed to equate to μA/cm^2. Mathias et al. (14) showed the Na^+-flux between pipette and cell scales with the pipette tip resistance R_P (Ω), which has also been measured as described near Fig. 3. Thus, the information was available to estimate the actual value of $[Na^+]_i$ using this equation, which was derived in Mathias et al. (14),

$$[Na^+]_i = [Na^+]_P - (3I_p - I_{inb})R_P/FD\rho,$$

where D (1.5×10^{-5} cm^2/s) is the diffusion coefficient for Na^+, and ρ (60 Ω−cm) is the resistivity of the pipette solution.

Fig. 6 *B* graphs I_{inb} versus our estimates of $[Na^+]_i$. There was no significant difference between EPI and ENDO in the measured values of I_{inb} ($p = 0.5$). We estimated the Na^+ permeability (P_{Na}) from the Goldman (constant field) equation

$$I_{inb} = F P_{Na}\phi([Na^+]_i e^{\phi} - [Na^+]_o)/(e^{\phi} - 1), \phi = FV_m/RT.$$

P_{Na} was 1.6×10^{-8} cm/s in either EPI or ENDO myocytes. As mentioned above, removal of external Na^+ should have revealed the small outward Na^+-current (I_{outb}), which is given by

$$I_{outb} = FP_{Na}\phi[Na^+]_i e^{\phi}/(e^{\phi} - 1).$$

The calculated value I_{outb} at $[Na^+]_i = 100$ mM and $\psi_i = -60$ mV is 0.03 pA/pF, which is ~5% of I_{inb}. At physiological values of $[Na^+]_i$, the value of I_{outb} would be ~10-fold smaller.

We also measured the dependence of I_P on $[Na]_i$. This is plotted for EPI and ENDO myocytes in Fig. 6 *C*. The smooth curves are the best fit with the following equation, which describes activation by three independent and identical Na^+-binding sites (13):

$$I_P = I_{max}([Na]_i/([Na]_i + K_{Na}))^3.$$

I_{max} was 0.48 pA/pF and K_{Na} was 2.6 mM in EPI myocytes, whereas I_{max} was 0.27 pA/pF and K_{Na} was 2.6 mM in ENDO myocytes. The half-saturating Na^+-concentrations were 9.4 mM in EPI and 9.8 mM in ENDO myocytes. Thus the dependence of I_P on bulk $[Na^+]_i$ was not different in the two regions. There have been, however, reports of a local restricted subsarcolemma space in which the local concentration of Na^+ differs from bulk $[Na^+]_i$ (15). One characteristic of such a space is that the larger the value of I_P, the greater the depletion of local Na^+. Since I_P in EPI is twice as large as in ENDO, although their dependences on bulk $[Na^+]_i$ were the same, these data suggest the absence of a restricted subsarcolemmal space. However, when the corrections were made for differences between bulk pipette and internal Na^+, the correction for EPI was generally larger owing to the larger value of I_P. The main conclusion of this part of our study is that differences in sensitivity to bulk $[Na^+]_i$ cannot account for the differences in maximum I_P.

$[Na^+]_i$ in EPI, MID, and ENDO myocytes

Since I_{inb} is approximately the same in EPI and ENDO whereas the maximum I_P is approximately twofold larger in EPI than ENDO, resting $[Na]_i$ may be significantly smaller in EPI than ENDO. We therefore used the Na^+-sensitive dye SBFI to directly estimate $[Na^+]_i$ in the different types of cells (see Methods). The average values of resting $[Na^+]_i$ given in Fig. 7 *A* are 7 ± 2 mM in EPI (31 cells from six dogs), 9 ± 3 mM in MID (22 cells from three dogs), and 12 ± 3 mM in ENDO (29 cells from six dogs). There is a significant effect of position ($p < 0.01$). Mean $[Na^+]_i$ at each position was significantly different from that at any other position ($p < 0.05$). Thus $[Na^+]_i$ is indeed significantly smaller in EPI than ENDO, and there appears to be a transmural gradient in $[Na^+]_i$. In a resting myocyte, I_{inb} is probably the dominant influx pathway for Na^+; however, in the contracting heart, other pathways will come into play, and these pathways could differ in the different cell types. We therefore recorded $[Na^+]_i$ in paced myocytes.

Fig. 7 *B* shows the time-course of changes in $[Na^+]_i$ when a MID cell was paced at 1 Hz and 2 Hz. The time-course for EPI and ENDO cells were similar to that shown. $[Na^+]_i$ clearly increases with increases in the rate of pacing, but as shown by many others, it requires several minutes to achieve a new steady state, hence the changes are slow relative to the time-course of an action potential. Fig. 7 *C* shows the steady-state values of $[Na^+]_i$ when the cells were paced at 2 Hz. The values obtained from two dogs were 9 ± 2 mM in EPI (10 cells), 11 ± 2 mM in MID (nine cells), and 14 ± 3 mM in ENDO (10 cells). There was a significant effect of position ($p < 0.001$). EPI differed from ENDO ($p < 0.05$) and MID differed from ENDO ($p < 0.05$). Thus, pacing the cells caused an increase in $[Na^+]_i$ in each region, but did not alter the transmural gradient.

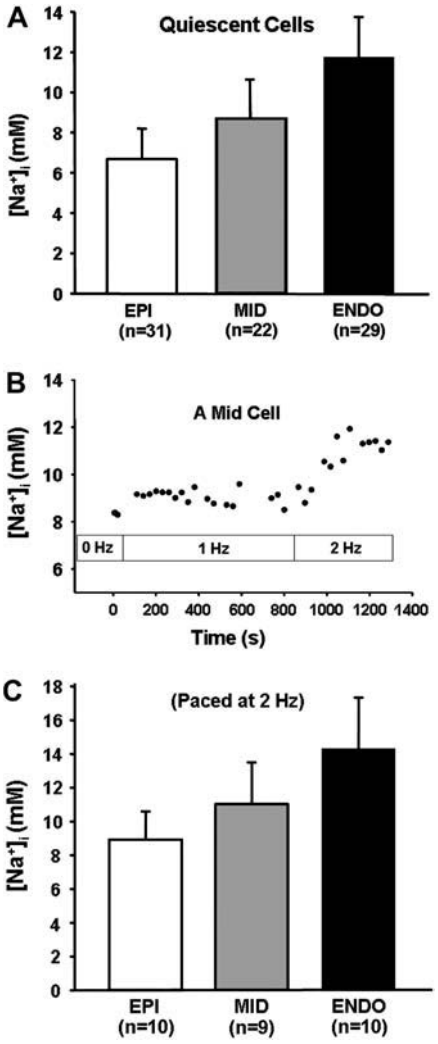

FIGURE 7 Measurements of $[Na^+]_i$ in EPI, MID, and ENDO myocytes. Based on the data in Fig. 6, $[Na^+]_i$ is expected to be higher in ENDO than EPI cells. To test this hypothesis, we measured $[Na^+]_i$ using the Na^+-sensitive dye SBFI. (*A*) Values of $[Na^+]_i$ in quiescent myocytes from EPI, MID, and ENDO regions of the left ventricular wall. Ratios were measured as described in Methods and $[Na^+]_i$ was determined from the calibration curve shown in Fig. 2. (*B*) Changes in $[Na^+]_i$ with pacing. This MID cell was stimulated to contract at the indicated rates with field electrodes. With increases in the rate of stimulation, $[Na^+]_i$ increased over a time period of 100–200 s. (*C*) Average values of $[Na^+]_i$ in EPI, MID, and ENDO myocytes paced at 2 Hz. The effect of pacing was to increase $[Na^+]_i$ in each domain, but the significantly higher $[Na^+]_i$ in ENDO than EPI (see text) is similar to that seen in quiescent cells, consistent with the highest I_P in EPI and lowest in ENDO.

DISCUSSION

There has been intensive investigation of the biophysical and molecular differences in I_{to1} among ENDO, MID, and EPI (2,16,17). In addition, one recent article (18) suggests that ENDO myocytes may have significantly larger T- and L-type Ca^{2+}-currents than EPI; however, Cordeiro et al. (19) did not find differences in L-type currents. Nevertheless, the differences in action-potential morphology will lead to differences

in Ca^{2+} entry. The studies reported here suggest that, other than differences in I_{to1} and Ca^{2+}-entry, there are differences in the restorative processes that balance ion fluxes through the other membrane channels. The major results are:

1. There is a transmural gradient in Na/K pump activity, with the maximum activity of EPI myocytes being roughly twice that of ENDO.
2. The transmural gradient in I_P is due to the maximum turnover rate, which could be either a higher density of Na/K pump protein or a higher turnover rate of each pump protein in EPI relative to MID relative to ENDO.
3. The inward background Na^+-currents are approximately the same in EPI and ENDO myocytes; hence, in physiological conditions, I_P will be nearly the same in ENDO and EPI, but the value of $[Na^+]_i$ in ENDO will be almost twice as high as in EPI, as indicated by the SBFI data.
4. Because of the transmural gradient in $[Na^+]_i$, I_P is nearly the same in the three regions; hence, it should have little, if any effect on action-potential duration. However, in physiological conditions, the lower $[Na^+]_i$ in EPI means these myocytes have a higher capacity for Na/Ca exchange.

The above stated conclusions are based on data from isolated cells, whereas the ventricular wall is a syncytium, with all cells in communication via low resistance gap junctions. In the Appendix we estimate the effect on baseline $[Na^+]_i$ of diffusion via gap junctions between regions with different values of maximum I_P. The conclusion is that diffusion is only important in a relatively small region of cells at the border where maximum I_P changes. In the majority of cells, the value $[Na^+]_i$ will be the same as in isolated myocytes.

Unanswered questions

Our previous studies have suggested the coexistence of two isoforms of the Na/K ATPase α-subunit in canine EPI myocytes, one with high DHO affinity ($\sim$1 μM, probably the α_3-isoform) and one with much lower DHO affinity ($\sim$70 μM, probably the α_1-isoform) (13,20). The present experiments did not focus on whether the differences in total pump current reflect differential expression of these isoforms. However, we have found that the $[K^+]_o$-affinity of the α_1-isoform in heart is much lower than that of either the α_2- or α_3-isoform (13,20). Hence, the observation in Fig. 4 that increasing $[K^+]_o$ from 5.4 mM to 15 mM caused an $\sim$30% increase in either I_P(EPI) or I_P(ENDO) suggests that each of the two cell types predominantly expresses the α_1-isoform. For example, if either EPI or ENDO myocytes expressed only the α_3-isoform, increasing $[K^+]_o$ from 5.4 mM to 15 mM should have had no significant effect on I_p, whereas if either expressed only the α_1-isoform, I_p should have increased by $\sim$40%. A distribution of $\sim$70% α_1-isoform and 30% α_3-isoform is consistent with our observation, but more data are needed to provide an accurate estimate. Nevertheless, assuming that each region predominantly expresses the α_1-isoform, the gradient in maximum I_p (EPI $>$ MID $>$ ENDO) may reflect either a higher density or a higher maximum turnover rate of the α_1-isoform. The former implies differential regulation of protein expression whereas the latter implies differential post-translational modifications of the pump proteins. Either is possible, and it would be useful to know which is responsible for the recorded difference.

Finally, previous studies have suggested that the differences in I_{to1} between ENDO and EPI myocytes in canine heart are under the tonic influence of the renin-angiotensin system (3). Incubation of EPI myocytes with angiotensin II for 2–52 h converted the properties of I_{to1} to those found in ENDO myocytes (lower density and slower recovery from inactivation), whereas incubation of ENDO myocytes with the angiotensin type 1a receptor blocker losartan converted the properties of I_{to1} found in ENDO to those found in EPI myocytes (higher density and faster recovery from inactivation). We are currently investigating whether a similar switch in maximum Na/K pump current can be induced by angiotensin II, and if so, by what mechanism.

APPENDIX

In the main body of this article we have estimated $[Na^+]_i$ and found a significantly lower value in EPI than ENDO cells. These measurements, however, were in isolated cells, whereas ventricular muscle is a syncytium with all cells being in communication via low resistance gap junctions. The purpose of this Appendix is to examine the effect of diffusion of Na^+ through gap junctions on the distribution of $[Na^+]_i$ across the ventricular wall, assuming a nonuniform distribution of I_P. We address the question of whether Na^+-diffusion is a major or minor determinant of $[Na^+]_i$. To do so, we assume there are three zones of tissue whose cells would sit at different values of $[Na^+]_i$ if they were isolated. When these zones are in communication via low-resistance gap junctions, the diffusion of Na^+ will tend to even out $[Na^+]_i$. In one limiting situation, if the length constant for diffusion of Na^+ is long relative to the dimensions of the myocardial wall, $[Na^+]_i$ in all cells could approach the same average value. In the other limiting situation, the length constant for diffusion of Na^+ could be very short in comparison to the dimensions of the zones and there will be almost a step change in $[Na^+]_i$ from one zone to the adjacent zone. The calculations here suggest the latter situation is more representative of the ventricles from the heart of any large mammal.

The analysis begins by defining a small cuboid of tissue, which contains several cells, but its dimension Δx is small relative to the length constant for Na^+-diffusion. Define the cell to cell Na^+-flux as $j(x)$ (moles/cm^2/s). The flux entering the left-hand side of the cuboid is then $\Delta x^2 j(x)$, and that leaving the right-hand side is $\Delta x^2 j(x + \Delta x)$. The transmembrane Na^+-flux within the cuboid is given by $\Delta x^3 (S_m/V_T) j_m$, where S_m/V_T (cm^{-1}) is the average surface area of membrane in a unit volume of tissue and j_m (moles/cm^2/s) is the transmembrane flux density. The intracellular Na^+-flux due to diffusion is given by

$$j(x) = -D_{Na} \frac{d[Na^+]_i}{dx},$$

and the transmembrane flux is

$$j_m = (3I_P - I_{Na})/F,$$

where $F = 10^5$ Coulombs/mole is the Faraday constant and I_{Na} is the total passive influx of Na^+, which includes I_{inb} plus electrically silent influx. The fluxes entering and leaving the cells within the cuboid must add to zero, yielding

$$D_{Na}\frac{d^2[Na^+]_i}{dx^2} = \frac{S_m}{V_T}(3I_P - I_{Na})/F. \quad (A1)$$

Eq. A1 can be made specific for different zones (EPI, MID, or ENDO) by inserting the appropriate definition of I_P, which has been experimentally determined in the main article. The values of the effective intracellular diffusion coefficient D_{Na} and the surface/volume ratio S_m/V_T need to be estimated.

With regard to S_m/V_T, the ventricular myocytes are typically 16 μm in diameter and 100 μm in length, giving a volume of 2×10^{-8} cm^3. They have a total capacitance of ~200 pF, so assuming a specific membrane capacitance of 1 μF/cm^2, their surface area of membrane is $\sim 200 \times 10^{-6}$ cm^2. Most of the ventricular volume is filled with cells and the literature provides estimates of the extracellular volume fraction at 20–30%. Using a value of 25% yields

$$\frac{S_m}{V_T} = 8000\,\text{cm}^{-1}.$$

With regard to D_{Na}, it should scale with the effective intracellular resistivity. Cohen et al. (21) reported that the longitudinal (from cell to cell along the axis of the cells) resistivity is ~500 Ω−cm. Spach et al. (22) reported that the propagation velocity is three- to fourfold slower in the transverse (across the ventricular wall perpendicular to the axis of the cells) direction relative to the longitudinal direction. Since propagation velocity depends on the square-root of the resistivity, this would imply the transverse resistivity is approximately 10-fold larger than the longitudinal resistivity, giving a value of 5000 Ω−cm. Cytoplasmic resistivity is on the order of 100 Ω−cm, so gap junctions have increased the effective longitudinal resistivity by approximately fivefold, and the transverse resistivity by approximately 50-fold. Applying this to the transverse diffusion of Na^+, for a cytoplasmic diffusion coefficient of $\sim 10^{-5}$ cm^2/s,

$$D_{Na} = 2 \times 10^{-7}\text{cm}^2/\text{s}.$$

Next consider the description of I_P in the different zones (ENDO, MID, and EPI denoted with 1, 2, and 3 respectively):

$$I_{P1,2,3} = I_{max1,2,3}\left(\frac{[Na^+]_i}{[Na^+]_i + K_{Na}}\right)^3. \quad (A2)$$

To analytically solve the differential equations, the dependence of I_P on $[Na^+]_i$ needs to be linearized, so Eq. A2 is expanded in a Taylor series around a convenient middle value of $[\underline{Na}^+]_i$ to obtain

$$I_{P1,2,3} \approx I_{P1,2,3}([\underline{Na}^+]_i) + \frac{dI_{P1,2,3}([\underline{Na}^+]_i)}{d[Na^+]_i}[[Na^+]_i - [\underline{Na}^+]_i]. \quad (A3)$$

If we choose $[\underline{Na}^+]_i = 10$ mM, over the range 7 mM $< [Na^+]_i <$ 12 mM, the value of I_P calculated with Eq. A3 is within 5% of that calculated with Eq. A2. Inserting the approximation given in Eq. A3 into Eq. A1, the final equations have the form

$$\frac{d^2[Na^+]_i}{dx^2} = \frac{1}{\lambda^2_{1,2,3}}([Na^+]_i - [Na^+]_{1,2,3}), \quad (A4)$$

where λ(cm) is the length constant:

$$\frac{1}{\lambda^2_{1,2,3}} = \frac{1}{FD_{Na}}\frac{S_m}{V_T}\frac{dI_{P1,2,3}([\underline{Na}^+]_i)}{d[Na^+]_i}. \quad (A5)$$

The values of $[Na^+]_{1,2,3}$ can be written in terms of the transport parameters; however, these are, by definition, the values when there is no gradient, as in isolated cells; hence, they have been experimentally measured:

$$[Na^+]_1 = 12\,\text{mM}\ [Na^+]_2 = 9\,\text{mM}\ [Na^+]_3 = 7\,\text{mM}.$$

The linearized version of the model in Eq. A2 gives

$$\frac{dI_{P1,2,3}([\underline{Na}^+]_i)}{d[Na^+]_i} = 3I_{max1,2,3}\frac{K_{Na}[\underline{Na}^+]_i^2}{([\underline{Na}^+]_i + K)^4}. \quad (A6)$$

Based on data in Fig. 6, $K_{Na} = 2.6$ mM, and based on data in Fig. 3, $I_{max1} = 0.63$ μA/cm^2, $I_{max2} = 0.50$ μA/cm^2, and $I_{max3} = 0.29$ μA/cm^2. Using these values, with the previous estimates of surface/volume ratio and effective transverse diffusion coefficient, the length constants are

$$\lambda_1 = 167\,\mu\text{m}\ \lambda_2 = 128\,\mu\text{m}\ \lambda_3 = 113\,\mu\text{m}.$$

These length constants are for pure transverse diffusion; however, the orientation of the fibers may not exactly parallel the wall of the ventricle, so there could be some component of longitudinal diffusion in the movement of Na^+ across the wall. The longitudinal diffusion coefficient was estimated to

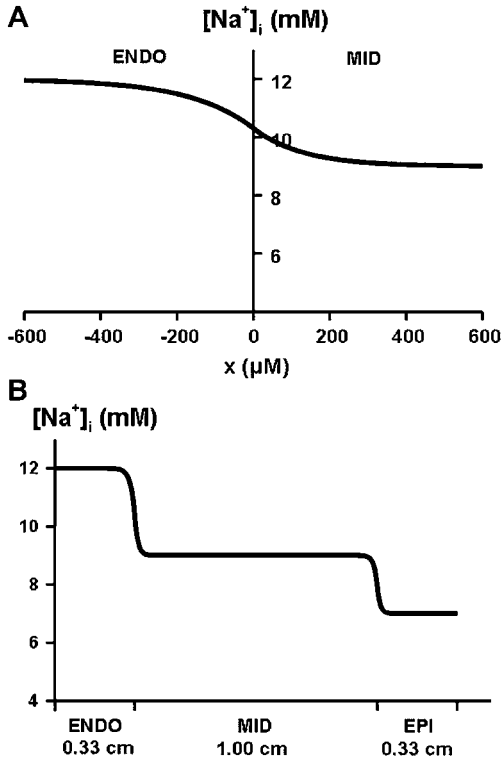

FIGURE 8 Calculations of Na^+ diffusion across the ventricular wall. The model uses the measured maximum values of I_P in EPI, MID, and ENDO and the measured dependence of I_P on $[Na^+]_i$. (*A*) The predicted distribution of $[Na^+]_i$ at the boundary between the ENDO and MID regions of the ventricular wall. The calculated $[Na^+]_i$ assumes that maximum I_P is smaller in zone 1 (ENDO) than zone 2 (MID), whereas the inward leak of sodium is the same. Parameter values were selected based on data in the main article. (*B*) The predicted distribution of $[Na^+]_i$ across the ventricular wall. The model utilizes data presented in the main article for isolated cells from ENDO, MID, and EPI. The conclusion is that cell-to-cell diffusion through gap junctions would impact relatively few cells, and the majority of cells would have an $[Na^+]_i$ that is determined by their local transport parameters rather than diffusion.

be 10-fold greater than that for transverse diffusion, hence the longitudinal length constants are approximately threefold longer (square-root of 10), which would not change any of the conclusions below.

The transverse length constants are indeed large relative to the cell diameter of 16 μm, so our assumption that a small cuboid could be defined is self-consistent. Moreover, the length constants are small in comparison to the dimensions of ENDO (zone 1 ~ 0.33 cm), MID (zone 2 ~1.0 cm), and EPI (zone 3 ~ 0.33 cm). Thus the shortest zone with the longest length constant is ENDO, where the width of the zone is equivalent to $\sim 20\lambda_1$. Since concentration gradients depend exponentially on x/λ, the diffusional dimensions of the zones are effectively infinite. For simplicity, we will therefore solve for diffusion between two zones of infinite dimensions, to illustrate the concentration changes. Since the largest gradient in I_P is between ENDO and MID (zones 1 and 2), parameter values for these two zones are used in the graph shown in Fig. 8 *A*. The differential equation to be solved is given in Eq. A4. The boundary conditions need to be specified. Assume $x = 0$ is at the border between ENDO and MID, with positive x in MID. For continuity of the Na^+-concentration and -flux, the conditions at this boundary are

$$[Na^+]_i(0^-) = [Na^+]_i(0^+)$$
$$\frac{d[Na^+]_i(0^-)}{dx} = \frac{d[Na^+]_i(0^+)}{dx}. \quad \text{(A7)}$$

The boundary conditions at large x are

$$\lim_{x \to -\infty} [Na^+]_i(x) \to [Na^+]_1 \quad \lim_{x \to +\infty} [Na^+]_i(x) \to [Na^+]_2. \quad \text{(A8)}$$

Eq. A4 with these boundary conditions has the solution

$$[Na^+]_i(x) = \begin{cases} [Na^+]_1 + \dfrac{\lambda_1}{\lambda_2 + \lambda_1}([Na^+]_2 - [Na^+]_1)e^{x/\lambda_1} & x \le 0 \\ [Na^+]_2 - \dfrac{\lambda_2}{\lambda_2 + \lambda_1}([Na^+]_2 - [Na^+]_1)e^{-x/\lambda_2} & x \ge 0 \end{cases}. \quad \text{(A9)}$$

Fig. 8 *A* shows the transition between ENDO and MID over a distance of ± 600 μm. The distribution across the ventricular wall is graphed in Fig. 8 *B*. On the scale of the ventricular wall, the changes in concentration are almost step functions. Thus, it appears that diffusion of Na^+ from one region of the ventricle to another will not significantly affect the concentration in the majority of cells in either region.

This work was supported by the American Heart Association and by grants Nos. HL54031, HL20558, HL28958, and HL67101 from the National Heart, Lung and Blood Institute of the National Institutes of Health.

REFERENCES

1. Noble, D. 1979. Initiation of the Heartbeat, 2nd Ed. Oxford University Press, NY.
2. Antzelevitch, C., G.-X. Yan, W. Shimizu, and A. Burashnikov. 2000. Chapter 26: Electrical heterogeneity, the ECG, and cardiac arrhythmias. *In* Cardiac Electrophysiology. From Cell to Bedside, 3rd Ed. D.P. Zipes and J. Jalife, editors. W.B. Saunders, Philadelphia, PA. 222–238.
3. Yu, H., J. Gao, H. Wang, R. Wymore, S. Steinberg, D. McKinnon, M. R. Rosen, and I. S. Cohen. 2000. Effects of the renin-angiotensin system on the current I_{to} in epicardial and endocardial ventricular myocytes from the canine heart. *Circ. Res.* 86:1062–1068.
4. Liu, D. W., and C. Antzelevitch. 1995. Characteristics of the delayed rectifier current (I_{Kr} and I_{Ks}) in canine ventricular epicardial, midmyocardial, and endocardial myocytes. *Circ. Res.* 76:351–365.
5. Zygmunt, A. C., G. T. Eddlestone, G. P. Thomas, V. V. Nesterenko, and C. Antzelevitch. 2001. Larger late sodium conductance in M cells contributes to electrical heterogeneity in canine ventricle. *Am. J. Physiol.* 281:H689–H697.
6. Gao, J., I. S. Cohen, R. T. Mathias, and G. J. Baldo. 1998. Na^+ and Ca^{2+} transport in epicardial and endocardial ventricular myocytes. *Biophys. J.* 74:A160.
7. Cohen, I. S., N. B. Datyner, G. A. Gintant, N. K. Mulrine, and P. Pennefather. 1987. Properties of an electrogenic sodium-potassium pump in isolated canine Purkinje myocytes. *J. Physiol.* 383:251–267.
8. Yu, H., F. Chang, and I. S. Cohen. 1993. Pacemaker current exists in ventricular myocytes. *Circ. Res.* 72:232–236.
9. Fabiato, A. 1988. Computer programs for calculating total from specified free or free from specific total ionic concentrations in aqueous solutions containing multiple metals and ligands. *Methods Enzymol.* 157:378–417.
10. Gao, J., I. S. Cohen, R. T. Mathias, and G. J. Baldo. 1992. Isoprenaline, Ca^{2+} and the Na^+-K^+ pump in guinea-pig ventricular myocytes. *J. Physiol.* 449:689–704.
11. Diarra, A., C. Sheldon, and J. Church. 2001. In situ calibration and $[H^+]$ sensitivity of the fluorescent Na^+ indicator SBFI. *Am. J. Physiol. Cell Physiol.* 280:C1623–C1633.
12. Despa, S., M. A. Islam, S. M. Pogwizd, and D. M. Bers. 2002. Intracellular $[Na^+]$ and Na^+ pump rate in rat and rabbit ventricular myocytes. *J. Physiol.* 539:133–143.
13. Gao, J., I. S. Cohen, R. T. Mathias, and G. J. Baldo. 1995. Two functionally different Na/K pumps in cardiac ventricular myocytes. *J. Gen. Physiol.* 106:995–1030.
14. Mathias, R. T., I. S. Cohen, and C. Oliva. 1990. Limitations of the whole cell patch-clamp technique in the control of intracellular concentrations. *Biophys. J.* 58:759–770.
15. Despa, S., and D. M. Bers. 2003. Na/K pump current and $[Na]_i$ in rabbit ventricular myocytes: local $[Na]_i$ depletion and Na buffering. *Biophys. J.* 84:4157–4166.
16. Dixon, J. E., W. Shi, H.-S. Wang, C. McDonald, H. Yu, R. S. Wymore, I. S. Cohen, and D. McKinnon. 1996. Role of the Kv4.3 K^+ channel in ventricular muscle. A molecular correlate for the transient outward current. *Circ. Res.* 79:659–668.
17. Rosati, B., Z. Pan, S. Lypen, H.-S. Wang, I. S. Cohen, J. E. Dixon, and D. McKinnon. 2001. Regulation of KChIP2 potassium channel β subunit gene expression underlies the gradient of transient outward current in canine and human ventricle. *J. Physiol.* 533:119–125.
18. Wang, H. S., and I. S. Cohen. 2003. Calcium channel heterogeneity in canine left ventricular myocytes. *J. Physiol.* 547:825–833.
19. Cordeiro, J. M., L. Greene, C. Heilmann, D. Antzelevitch, and C. Antzelevitch. 2004. Transmural heterogeneity of calcium activity and mechanical function in the canine left ventricle. *Am. J. Physiol. Heart Circ. Physiol.* 286:H1471–H1479.
20. Gao, J., R. S. Wymore, Y. Wang, G. R. Gaudette, I. B. Krukenkamp, I. S. Cohen, and R. T. Mathias. 2002. Isoform-specific stimulation of cardiac Na/K pumps by nanomolar concentrations of glycosides. *J. Gen. Physiol.* 119:297–312.
21. Cohen, I. S., R. T. Falk, and R. P. Kline. 1982. Voltage-clamp studies on the canine Purkinje strand. *Proc. R. Soc. Lond. B. Biol. Sci.* 217: 215–236.
22. Spach, M. S., J. F. Heidlage, and P. C. Dolber. 2000. Chapter 25: The dual nature of anisotropic discontinuous conduction in the heart. *In* Cardiac Electrophysiology. From Cell to Bedside, 3rd Ed. D.P. Zipes and J. Jalife, editors. W.B. Saunders, Philadelphia, PA. 213–222.